Eur. J. Biochem. **263**, 20–26 (1999) © FEBS 1999

The three-dimensional structure of Asp189Ser trypsin provides evidence for an inherent structural plasticity of the protease

Erika Szabó[1,2], Zsolt Böcskei[3], Gábor Náray-Szabó[3] and László Gráf[1]

[1]*Department of Biochemistry, Eötvös L. University, Budapest, Hungary;* [2]*Agricultural Biotechnology Center, Gödöllõ, Hungary;* [3]*Department of Theoretical Chemistry, Eötvös L. University, Budapest, Hungary*

Trypsin mutant Asp189Ser, first described by Gráf *et al*. [Gráf, L., Jancsó, Á., Szilágyi, L., Hegyi, G., Pintér, K., Náray-Szabó, G., Hepp, J., Medzihradszky, K. & Rutter, W.J. (1988) *Proc. Natl Acad. Sci. USA* **85**, 4961–4965] has played an important role in recent studies on the structural basis of substrate-specific catalysis by serine proteases. The present work reports the three-dimensional structure of this mutant crystallized in unliganded form: the first unliganded rat trypsin structure reported. The X-ray structure of the Asp189Ser trypsin mutant in complex with bovine pancreatic trypsin inhibitor is already known. The X-ray structure of free Asp189Ser rat trypsin revealed that the single amino acid mutation at the bottom of the substrate binding pocket of trypsin resulted in extensive structural changes around the mutated site and in dimerization of the mutant, in contrast with the complexed enzyme the structure of which is practically the same as that of wild-type trypsin. The structural rearrangement in the mutant was shown to be restricted to the activation domain region providing further evidence for the allosteric property of this structural–functional unit of the enzyme. This study supports our view that the plasticity of the activation domain may play an important role in the mechanism of substrate-specific serine protease action.

Keywords: activation domain; flexibility; plasticity; serine proteases; X-ray crystallography.

The exquisite substrate specificity of trypsin and chymotrypsin, coupled with the highly homologous structures of their substrate binding sites [1–7], has made this pair of enzymes ideal models for studying the mechanism of substrate-specific catalysis. The specificity difference between trypsin and chymotrypsin has long been thought to be due to the presence of the negative charge of Asp189 carboxylate (S1 residue) in the substrate binding pocket of trypsin (matching the positive charge of the P1 side chain in the substrate) and its absence in chymotrypsin [3]. Mutation of Asp189 in trypsin to serine (the corresponding residue in chymotrypsin), however, did not change the substrate specificity of trypsin to that of chymotrypsin but resulted in a poor, nonspecific protease [8]. The X-ray structure of the Asp189Ser rat trypsin mutant complexed with bovine pancreatic trypsin inhibitor (BPTI) and acetate was determined and revealed a structure almost identical to that of wild-type trypsin [9]. This result did not explain the impaired proteolytic activity of the mutant. Furthermore, there appeared to be a conflict with a previous prediction by Hedstrom *et al*. [10] who proposed, on the basis of inability of Asp189Ser rat trypsin to bind proflavin, that the substrate binding pocket of the mutant might be deformed. Our present determination of the X-ray structure of unliganded Asp189-Ser trypsin resolves this conflict by providing direct evidence for a deformed structure of the S1 binding site. Deformation of the structure of Asp189Ser trypsin relative to those of trypsin and chymotrypsin is not restricted to the specificity pocket, however, but extends to some parts of the activation domain. In this regard the Asp189Ser trypsin mutant and trypsinogen behave similarly as the activation domains of both proteins undergo structural transitions upon inhibitor binding [9,11].

Correspondence to L. Gráf, Department of Biochemistry, Eötvös L. University, Puskin u. 3. Budapest, H-1088, Hungary. Fax: +36 1 266 7830, Tel.: +36 1 266 7858, E-mail: graf@ludens.elte.hu

Abbreviations: BPTI, bovine pancreatic trypsin inhibitor.

(Received 26 January 1999, accepted 2 March 1999)

METHODS

Expression and purification of the recombinant protein

The Asp189Ser trypsin mutant was expressed in yeast, purified and activated as described previously [12]. The purity of the enzyme was analysed by SDS/PAGE. The enzyme concentration was determined by BioRad protein assay.

Crystallization and data collection

The uncomplexed Asp189Ser trypsin crystals were grown at 4 °C by the hanging-drop vapour diffusion method, using a protein concentration of approximately 10 mg·mL^{-1}, in 0.1 M sodium citrate buffer (pH 5.6), 10 mM $CaCl_2$, 22% poly-(ethylene glycol) 3350, 0.15 M ammonium chloride. All of the drops contained precipitate except one which contained a large plate-shaped crystal with dimensions 0.6 × 0.5 × 0.15 mm.

Intensity data were collected at room temperature on a Rigaku Raxis II imaging plate using a Rigaku RU200 generator. The radiation source was a normal focus copper rotating anode (λ = 1.5418 Å) equipped with a graphite monochromator and run at 40 kV and 150 mA. Data processing and reduction was carried out using the PROCESS package [13]. Unit cell dimensions are shown in Table 1 together with other data collection details.

Structure solution by molecular replacement

For molecular replacement calculations the model was taken from the protein data bank (entry PDB1BRB.ENT, rat trypsin

mutant Asp189Gly/Gly226Asp in complex with BPTI [14]). The inhibitor, the structurally bound waters as well as the two differing side chains, Asp189Ser and Gly226Asp were removed, leaving 1646 protein atoms.

AmoRe [15] as implemented in the CCP4 suite [16] was used to solve the structure of rat trypsin mutant Asp189Ser. The self rotation function clearly indicated the presence of a dimer in the asymmetric unit of the monoclinic cell, which was in accordance with an average V_M value of 2.07 $Å^3 \cdot g^{-1}$ calculated by assuming $Z = 4$ molecules in the unit cell.

Patterson functions for the model, used in rotation searches were calculated in an artificial triclinic cell with orthogonal axes of length 50 Å. Because the model was a monomer in a quite different space group, it was necessary to carry out cross-rotation searches with half of the content of the asymmetric unit. Despite this, two peaks related by a noncrystallographic twofold axes in the cross-rotation function were evident; one of them was used to find the corresponding translation component. A search on data from 10.0 to 4.0 Å resolution provided only one single peak in the translation function higher than its own half-height. The conventional *R* factor at this point was 50.5, and the correlation coefficient was 25.8. With this solution fixed, the second largest peak related by a twofold axis to the first was taken to test if its translation component could be found. A decrease in the *R*-factor to 43.2% (and an increase in the correlation coefficient to 46.7) indicated that molecular replacement probably provided a good solution.

Table 1. Crystallographic data and refinement parameters. Space group, $P2_1$; number of molecules in the asymmetric unit, 2; Unit cell, a = 45.92 Å, b = 49.79 Å, c = 89.88 Å, β = 97.3°; V_m, 2.07 $Å^3 \cdot Da^{-1}$.

	Overall	Highest bin
Data collection		
Resolution range (Å)	100–2.5	2.54–2.59
Number of unique reflections	13312	470
Data redundancy	3.1	3.0
Completeness (%)	94.5	91.9
Average I/σ(I[a])	7.7	2.6
R_{merge}[b]	0.120	0.296
Refinement		
Resolution range (Å)	100–2.5	
Number of reflections	12103	
Cut-off [σ(F)]	2	
R_{factor}[c]	0.182	
R_{free}	0.242	
Model		
Number of nonhydrogen atoms		
Protein	3328	
Calcium	2	
Water molecules	131	
Thermal parameters		
< B > for protein atoms	18.64 $Å^2$	
< B > for calcium ions	33.6 $Å^2$	
< B > for water molecules	25.8 $Å^2$	
Stereochemistry		
RMS deviations from ideal values:		
Bond lengths	0.007 Å	
Bond angles	1.369°	
Dihedral angles	26.173°	
Improper angles	1.304°	

[a] *I* is the intensity of the reflections. [b] $R_{merge} = \Sigma_{hkl}\Sigma_i (< I > - I_i)/\Sigma_{hkl}\Sigma_i I_i$. [c] $R_{factor} = \Sigma(F_{obs} - F_{calc})/\Sigma F_{obs}$.

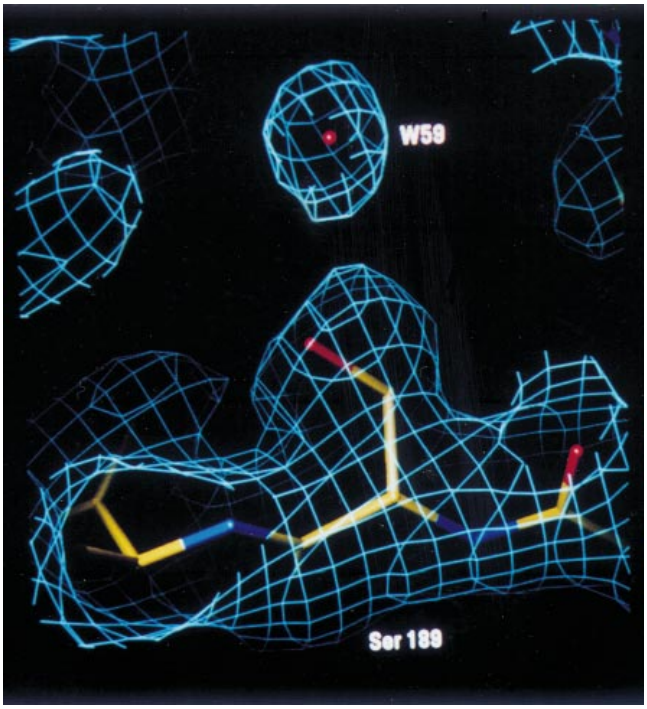

Fig. 1. 2Fo-Fc type map showing the position of the Ser189 residue with a nearby water molecule (W59) in the unliganded Asp189Ser rat trypsin mutant.

Rigid body refinement with the FITING routine of AMORE [15] converged with a conventional *R* factor of 33.6% (correlation coefficient, 70.2) for data from 10 to 4.0 Å resolution. The molecular replacement solution was tested for intermolecular contacts. One of the most important features of the Asp189Ser trypsin structure had already been noted at that time: two trypsin molecules were seen to form a dimer; members of the dimer complement each other's cavities nicely (see later). The only intermolecular bump was that between the tyrosine side chains of residues A217 and B217.

Refinement and model building

2Fo-Fc and Fo-Fc-type electron density maps were calculated and displayed at 2.6 Å resolution by O [17] on an SGI R4400

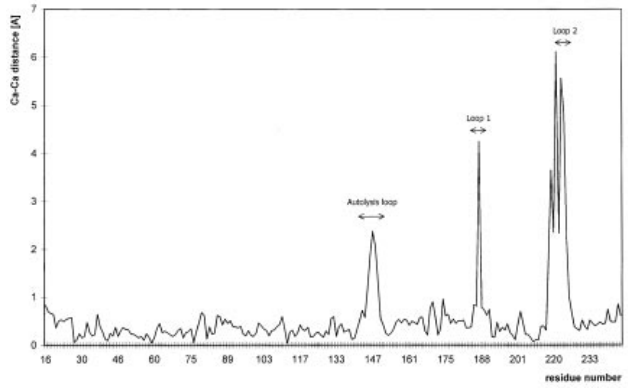

Fig. 2. Distance between corresponding Cα atoms in superposed structures of the unliganded Asp189Ser rat trypsin mutant and wild-type rat trypsin in complex with benzyldiamine (protein data bank code: 1ane).

workstation. The two clashing residues (A217 and B217) were replaced by alanines before difference Fourier maps were calculated. The difference Fourier maps indicated new positions for both side chains where no close contacts disturbed the structure any further. All of the four side chains (Lys97, Asp178, Asn202, Gln239) not seen in the model structure (PDB1BRB.ENT) due to disorder were visible in our structure. However, there was some ambiguity concerning the placement of the Ser189 side chains, so they were modelled as alanines. It was also evident from the density maps that a rearrangement of the regions A220–A225 and B220–B225 had taken place in this particular structure compared with other known structures; the corresponding density was weak and so no model building of these residues was attempted. XPLOR [18] refinement was carried out at 2.6 Å; this decreased the working *R*-factor from 0.393 to 0.240, while R_{free} decreased from 0.409 to 0.342. At this point there was sufficient density to allow the missing residues and Ser189 to be built. During refinement strict NCS (noncrystallographic symmetry) restraints were applied between molecules A and B. Figure 1 shows the position of the Ser189 side chain in the 2Fo-Fc-type map of the final model. The refinement statistics and parameters for the final structure are given in Table 1. The overall structure shows good stereochemistry; 81.9% of nonglycine residues are in their most favoured positions and 18.1% are in additional allowed regions of the Ramachandran plot as determined by PROCHECK [19]. The co-ordinates have been deposited in the Brookhaven protein data bank under the accession code 1amh.

Analysis of dimerization of bovine α-chymotrypsin and the Asp189Ser rat trypsin mutant by gel permeation chromatography

Analytical gel filtration experiments were performed on a computer-operated Pharmacia FPLC system equipped with an LC550 Plus controller and a UV MII monitor. Bovine α-chymotrypsin (Sigma) and highly purified recombinant Asp189Ser trypsin were run on a Superdex 75 HR 10/30 column at room temperature under the following conditions: injection volume, 50 μL; protein concentration, 20 mg·mL^{-1}; flow rate, 0.3 mL·min^{-1}; elution buffer, 0.15 M NaCl, 0.025 M sodium acetate, pH 4.0; detection at 280 nm. The column was calibrated by the following proteins (Sigma): BSA dimer (132 000) and monomer (66 000), ovalbumin (45 000), carbonic anhydrase monomer (29 000) and soybean trypsin inhibitor (20 000). The molecular masses of bovine α-chymotrypsin and the trypsin mutant were calculated by linear regression analysis of a plot of the $\log_{10} M_r$ vs. ratio of elution volume/void volume (V_e/V_o).

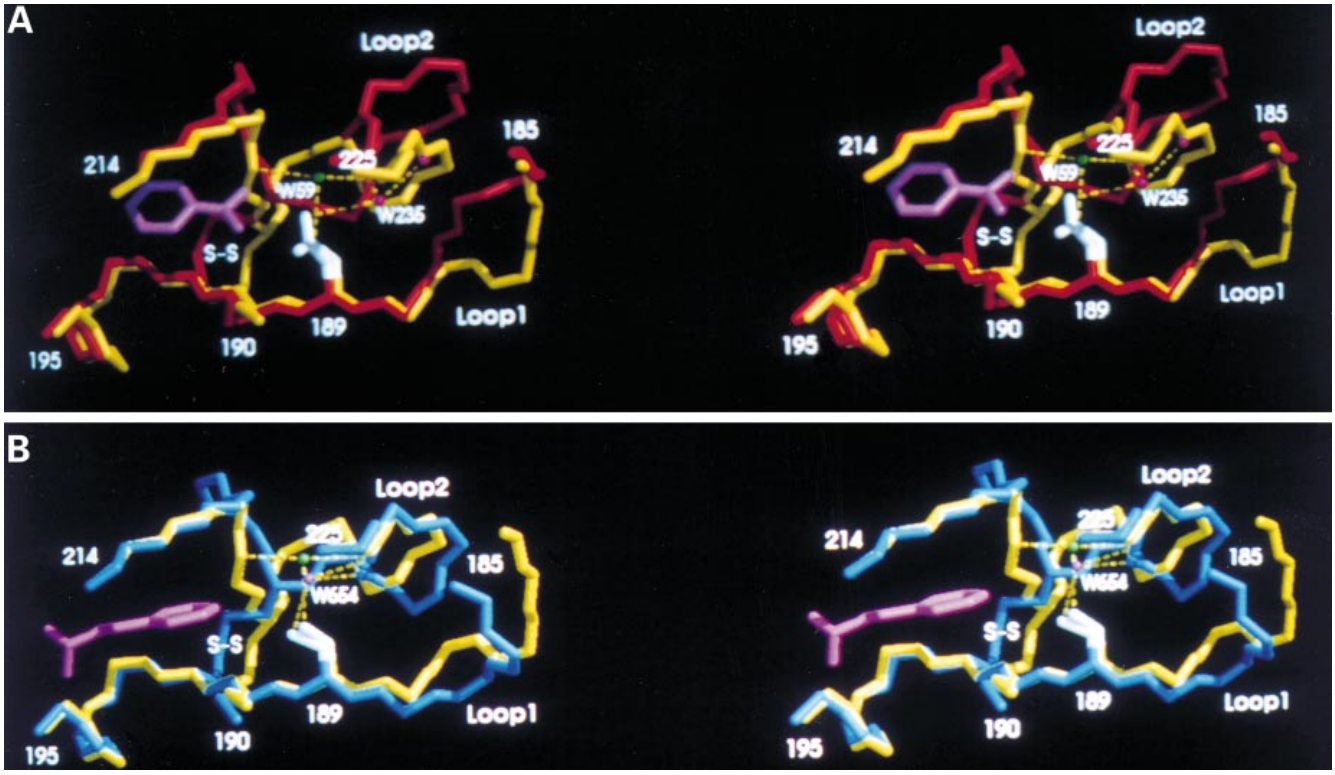

Fig. 3. Superposition of uncomplexed Asp189Ser rat trypsin with wild-type rat trypsin complexed with benzyldiamine and bovine α-chymotrypsin complexed with phenylethane boronic acid. (A) Stereo representation of the superposition of two segments (residues 185–195 and 214–225) of the uncomplexed Asp189Ser rat trypsin mutant (yellow) and wild-type rat trypsin complexed with benzyldiamine (red; protein data bank code: 1ane). Loop1 and loop2 denote the surface loops (Fig. 5A). The benzyldiamine (magenta) for trypsin is shown to mark the substrate specificity pocket. The side chains of 189 residues (Ser in Asp189Ser mutant, Asp in wild-type trypsin) are highlighted in white. Hydrogen-bonding interactions around the water molecules W235 (purple ball) in wild-type trypsin and W59 (green ball) in the mutant enzyme are indicated by dashed line. The disulphide bridge 191–220 (S–S) has different positions in the two proteases compared. (B) Stereo representation of the superposition of two segments (residues 185–195 and 214–225) of the uncomplexed Asp189Ser rat trypsin mutant (yellow) and bovine α-chymotrypsin complexed with phenylethane boronic acid (blue; 6cha [20]). Loop 1 and loop 2 denote the surface loops (Fig. 5A). The phenyl group of the inhibitor (magenta) for α-chymotrypsin is shown to mark the substrate specificity pocket. Hydrogen-bonding interactions around the water molecules W654 (purple ball) in wild-type chymotrypsin and W59 (green ball) in the mutant enzyme are indicated by dashed line. Disulphide bridge 191–220 (S–S) has different positions in the two proteases compared. The figures were drawn using program MidasPlus [21].

Average M_r for α-chymotrypsin and the trypsin mutant were 44 000 and 27 000 respectively, indicating that under our chromatography conditions chymotrypsin undergoes dimerization, while the prevalent form of the Asp189Ser rat trypsin mutant is a monomer.

RESULTS

Structural rearrangements in the surroundings of the mutation: comparison of the structure of the mutant to those of wild-type trypsin and chymotrypsin

The unliganded Asp189Ser mutant displays extensive structural changes as compared with wild-type trypsin (Fig. 2). As shown in the figure, the most striking rearrangements occurred in a part of the autolysis loop (residues 144–149), surface loop 1 (residues 185–188), surface loop 2 (residues 221–225) and residues 217–220 of the substrate binding pocket (the relationship of these regions with the activation domain is discussed later).

Comparison of parts of the substrate binding pockets and the surface loops of Asp189Ser rat trypsin and wild-type rat trypsin complexed with benzyldiamine (Fig. 3A) demonstrates that the newly introduced Ser189 side chain in the unliganded mutant occupies a position similar to that of Asp189 in the wild-type enzyme (the three-dimensional structure of the Asp189Ser trypsin mutant in complex with BPTI is not available in the Brookhaven data bank). The 189 residues point into the substrate binding pocket. As Fig. 3A illustrates, the Ser189 OH of the free Asp189Ser trypsin forms a hydrogen bond with a water molecule (W59), which appears to play a central role in mediating a contact between the S1 pocket (Gly219) and loop2 (Asn224); this interaction is missing in both wild-type trypsin and chymotrypsin. The W59 water may play a role similar to that of W235 in the structure of complexed wild-type trypsin. The hydrogen bond partners of W235 in wild-type trypsin are: Asp189 OD2, Asn224 O, W261. The distance between the two water molecules W59 and W235 in the superimposed structures is 3.1 Å, and the direction of the shift of W59 is towards the pocket.

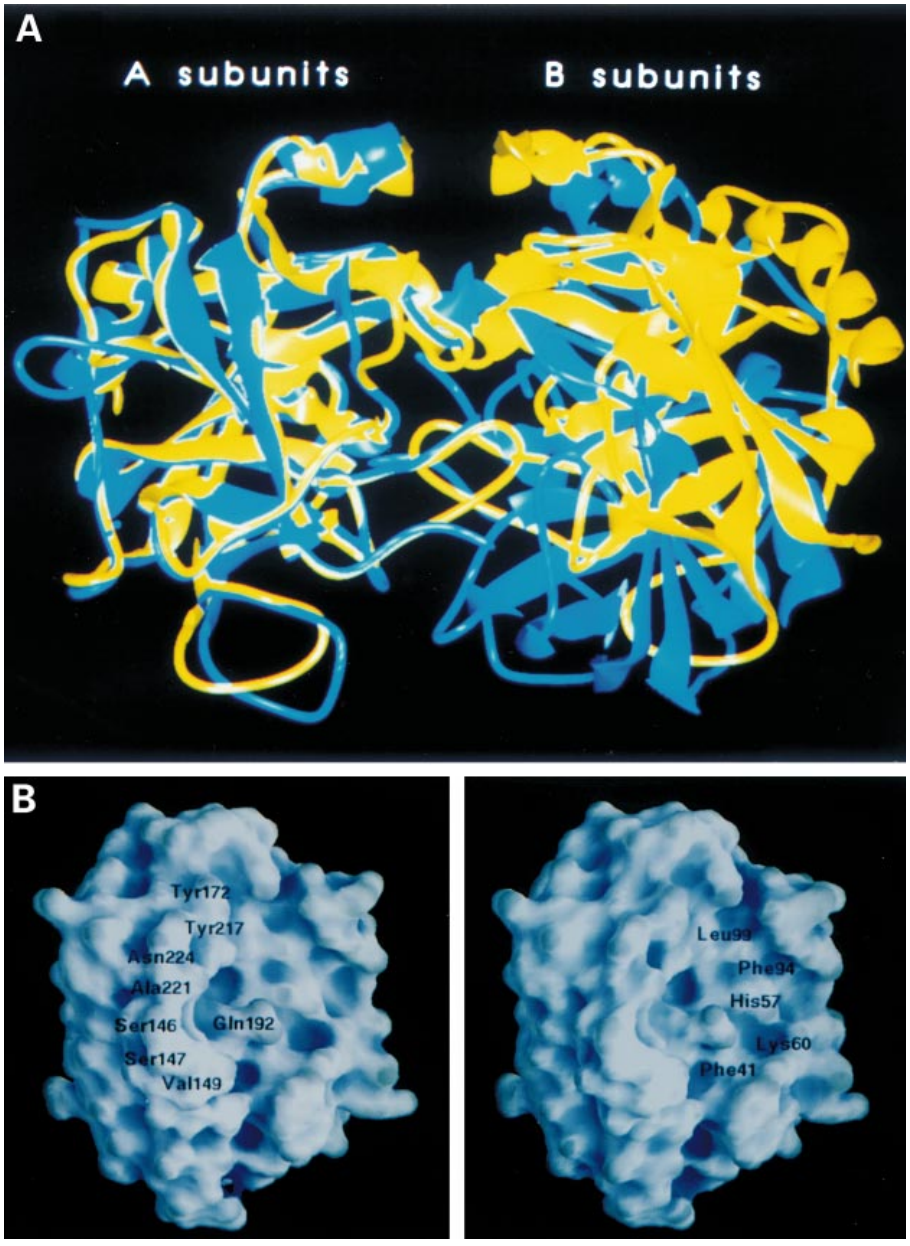

Fig. 4. The Asp189Ser rat trypsin dimer. (A) Ribbon diagram of the structure of free Asp189Ser rat trypsin (yellow, this study) aligned with that of bovine α-chymotrypsin complexed with phenylethane boronic acid (blue; protein data base code 6cha [20]). The figure was drawn using the program MidasPlus [21]. (B) Surface curvature representation of the Asp189Ser trypsin molecule. The A and B subunits (left and right respectively) are rotated around the *y*-axis by −90 ° and 90 ° respectively. The figure was calculated and displayed with the aid of program GRASP [25].

Table 2. Hydrogen bond interactions on the dimerization surfaces of the α-chymotrypsin and the Asp189Ser trypsin mutant. Superscript *a*, superscript *s* and superscript *l* refer to autolysis loop, substrate specificity pocket residues and a loop2 residue, respectively. A and B designate the subunits of dimers. As the monomers are related by a local two-fold axis, the hydrogen bonds can form in a reciprocating manner between the independent monomers A—B and B—A.

α-Chymotrypsin [24]			Asp189Ser rat trypsin mutant (this study)		
A146^a Tyr O	—	B57 His O	A147^a Ser OG	—	B57 His O
A146^a Tyr O	—	B57 His NE2	A148^a Gly N	—	B41 Phe O
A146^a Tyr OH	—	B214^s Ser O	A192^s Gln NE2	—	B145^a Leu O
A149^a Ala N	—	B59 Gly O	A192^s Gln NE2	—	B148^a Gly O
A149^a Ala N	—	B64 Asp OD1	A217^s Tyr OH	—	B175 Lys NZ
A150 Asn ND2	—	B57 His O	A221^l Ala N	—	B192^s Gln OE1
A151 Thr OG1	—	B35 Asp OD1			
A218^s Ser OG	—	B216^s Gly N			
A218^s Ser OG	—	B216^s Gly O			

In our Asp189Ser mutant structure there is an interesting reorganization of loop 2 and an apparently co-operative, but less characteristic rearrangement of loop 1 (Fig. 3A). As a result the Cα of Gly187 is shifted by 4.2 Å, but the ends of loop 1 remain unchanged. After this transition, the new loop structures are connected by a hydrogen bond between Gly188 N and Asp223 OD1. This bond is not present in the structure of the wild-type rat trypsin in which the distance of these atoms is 10.5 Å. The newly formed H-bond compensates for another one, between Ala221 O and Gly188 N in wild-type trypsin, that is lost as a consequence of the loop rearrangements.

Superposition of the substrate binding pockets and the surface loops of the Asp189Ser mutant trypsin and wild-type chymotrypsin can be seen in Fig. 3B, similar to the comparison of the same mutant to wild-type trypsin in the Fig. 3A. A water molecule (W654; hydrogen bond partners: Ser189 OG, Ser221 O, Thr224 O) in the bovine chymotrypsin structure with interactions similar to those of W59 in the Asp189Ser trypsin mutant, is also present in this region (Fig. 3B). Water molecule W59 is positioned in a way more similar to that of W654 of chymotrypsin than to W235 in trypsin. Accordingly, the distance between the two water molecules W59 and W654 in the superimposed structures is only 1.1 Å. Further chymotrypsin-like features of the Asp189Ser trypsin mutant are the conformation of loop 2 and the position of the side chain of Ser190 (compare Fig. 3A and 3B). The side chains of Ser190 in both the Asp189Ser trypsin mutant and chymotrypsin form a H-bond with the OH group of Tyr228 (data not shown).

Conformation of residues 217–220 of the substrate binding pocket of the mutant also changes (Fig. 3A and B) as compared with wild-type trypsin and chymotrypsin, probably due to the necessary rearrangement of the Tyr217 residues during dimer formation (see later). This change leads to a significant rearrangement of the Cys191–Cys220 disulphide bridge. The conformations of the remaining five cysteines are practically identical in the structures compared.

Chymotrypsin-like dimer formation

Unlike all trypsin variants examined so far our mutant crystallized as a dimer – a property of α-chymotrypsin [22]. Structural superposition of dimers of the Asp189Ser rat trypsin mutant and bovine α-chymotrypsin shows some similarity of the two assemblies (Fig. 4A). In both cases residues of the autolysis loops and the substrate specificity pockets are involved in dimerization, but the actual interactions are different. This is partly due to sequence differences in these regions between the two proteins and to the structural difference caused by the autoproteolytically cleaved state of the autolysis loop in chymotrypsin. Spontaneous cleavage of the tyrosine–threonine (residues 146–147) peptide bond in bovine α-chymotrypsin A liberates a new terminal carboxylate group that interacts electrostatically with the imidazole ring of His57 of the other subunit [23,24]. The two symmetric salt bridges between the chymotrypsin subunits are enforced by two symmetric sets of H-bonds (Table 2). In addition to forming H-bonds, Tyr146 of chymotrypsin fills a hole on the dimer interface [24]. In contrast, the structure of the Asp189Ser trypsin mutant (where a serine replaces Tyr146 of chymotrypsin) contains only poorly ordered low occupancy waters in this region. Steric complementarity between the dimerization surfaces of the two subunits in the trypsin mutant dimer is illustrated in Fig. 4B.

DISCUSSION

One important conclusion that may be drawn from the comparison of the structure of unliganded Asp189Ser trypsin with those of wild-type trypsin and chymotrypsin is that the replacement by serine of Asp189 in trypsin induced a considerable structural transition of parts of the autolysis loop (residues 144–149), surface loop 1 (residues 185–188), surface loop 2 (residues 221–225) and the substrate binding pocket (residues 217–220) (Fig. 2 and Fig. 3A and B). The altered structure is different from the corresponding ones in both native trypsin and chymotrypsin and may explain why the mutant enzyme exhibits no significant proteolytic activity. In this context it is interesting to note that conversion of the specificity of trypsin to that of chymotrypsin required, in addition to the rational modifications in the substrate binding pocket, the substitution of 11 amino acids at sites distant from the S1 specificity pocket [8,26,27]. Nine of these 11 sites are located in the two surface loops, loop 1 (residues 185–188) and 2 (residues 221–225) of the trypsin structure [26,27]. It has been proposed that these elements distant from the substrate binding and catalytic sites of the enzyme may modulate the conformational plasticity, as opposed to the static structure, of either the substrate binding site or the catalytic apparatus or, most probably, both [6,28]. A candidate for a structural unit that might mediate such conformational effects is the activation

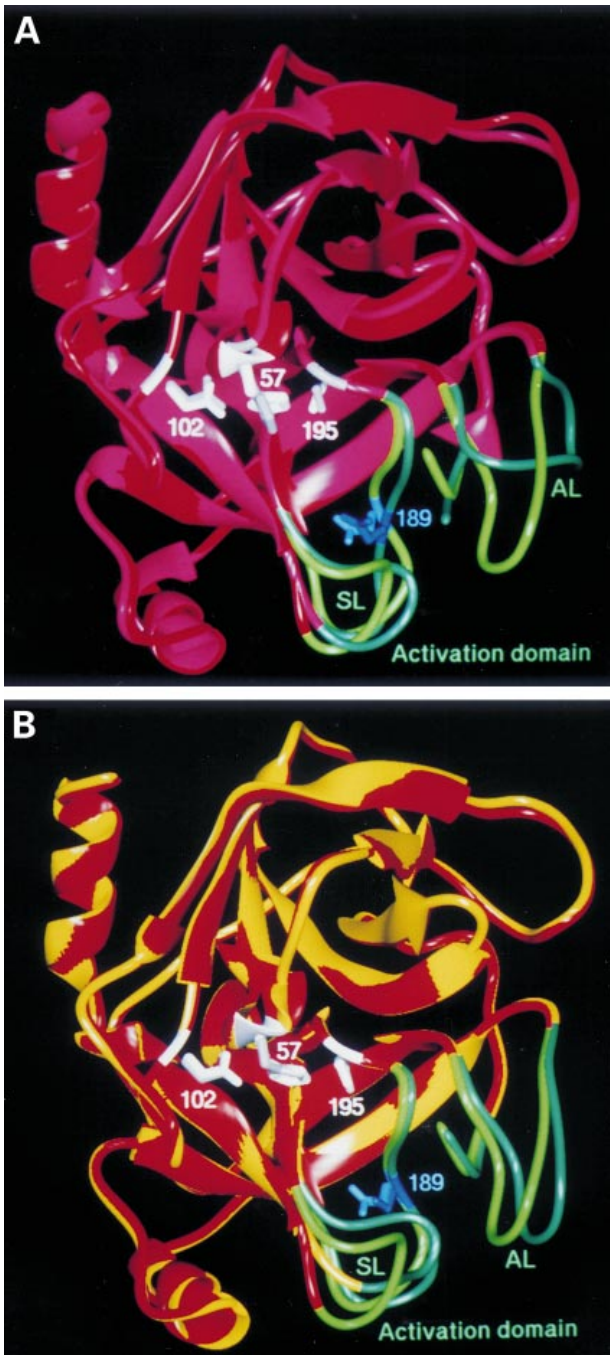

Fig. 5. Superposition of wild-type bovine trypsin and trypsinogen and of wild-type rat trypsin and unliganded Asp189Ser rat trypsin mutant. (A) Ribbon drawing of the superposition of wild-type bovine trypsin (red; protein data bank code: 1taw) and trypsinogen (dark purple; protein data bank code: 2tgd) structures. Colour codes for catalytic triad (His57, Asp102, Ser195): white in trypsin, grey in trypsinogen; for activation domain: green in trypsin, dark green in trypsinogen; for residue Asp189: blue in trypsin, dark blue in trypsinogen. SL and AL denote surface loops, and the autolysis loop, respectively. (B) Ribbon drawing of the superposition of wild-type rat trypsin (red; protein data bank code: 1ane) and unliganded Asp189Ser rat trypsin mutant (yellow; protein data bank code: 1amh) structures. Colour codes for catalytic triad (His57, Asp102, Ser195): white in wild-type, grey in the mutant trypsin; for activation domain: green in wild-type, dark green in the mutant trypsin; for residue Asp189: blue in wild-type, dark blue in the mutant trypsin. SL and AL denote surface loops, and the autolysis loop, respectively.

domain of these proteases [28]. The activation domain as originally defined and termed by Huber and Bode [29] consists of four sterically adjacent peptide segments (residues 16–19, 142–152, 184–193 and 216–223) (note that segment 142–152 is identical with the autolysis loop, whereas segments 184–193 and 216–223 partly comprise surface loops 1 and 2, respectively). These are organized differently and are more flexible in the zymogen forms than in the active proteases, but upon removal of the activation peptides they form apparently tightly packed structural units in the activated enzymes [29,30]. To visualize this difference the superposed three-dimensional structures of bovine trypsinogen and trypsin are shown in Fig. 5A. An analogous superposition of the structures of wild-type rat trypsin and unliganded Asp189Ser rat trypsin mutant is shown in Fig. 5B. It is clear from the comparison of these two figures that all conformational changes caused by the replacement of Asp189 with serine fall in the activation domain region of the enzyme (Fig. 5B). Furthermore, the conformational transition of unliganded Asp189Ser rat trypsin with BPTI [9] resembles the changes which occur during complexation of trypsinogen with BPTI and the isoleucine–valine dipeptide [11].

Whereas the Asp189Ser rat trypsin mutant was shown to be predominantly in monomeric form in solution it crystallized as a dimer. We have considered the question: does oligomerization have a functional relevance, or is only an artefact of crystallization? The accessible interface area calculated for the dimer of the Asp189Ser trypsin mutant is 2213 Å^2, larger than that for α-chymotrypsin (Table 3). According to a recent statistical analysis reported by Janin [31] only 1% of oligomeric interfaces in crystals have a contact area larger than 1600 Å^2. Based on statistics, it has been proposed that oligomerization resulting in crystal packing interfaces that exceed this value is of functional relevance, even if the oligomer structure is not detectable in solution [31]. Both bovine α-chymotrypsin and Asp189Ser trypsin satisfy this basic criterion for dimerization. The apparent lack of dimerization of the Asp189Ser trypsin mutant in solution may be due to the relatively smaller number of favourable H-bonding interactions of their subunits (Table 2) and the formation of some cavities, absent from the α-chymotrypsin structure [24], that are on the dimerization surface (Fig. 4B).

Is dimerization of the Asp189Ser rat trypsin mutant induced by structural rearrangements in the surroundings of the mutation, or does dimerization lead to these intramolecular conformational changes? If we assume that wild-type rat trypsin, similarly to bovine trypsin [5], does not tend to dimerize, then dimerization must be a consequence of an intramolecular structural rearrangement around the mutated site of Asp189Ser trypsin. This view is supported by the earlier work of Hedstrom *et al*. [10] who proposed, on the basis of the inability of the Asp189Ser rat trypsin mutant to bind proflavin,

Table 3. Accessible interface areas of trypsin and chymotrypsin/ogen dimers. Accessible interface areas were calculated with CCP4 [16] by using protein data base files 1trm for Asp102Asn rat trypsin, 2cga for chymotrypsinogen A, 6cha for α-chymotrypsin, 1amh for Asp189Ser rat trypsin.

Protein	Surface area [Å^2]
Asp102Asn rat trypsin	377
Chymotrypsinogen A	1086
α-Chymotrypsin	1995
Asp189Ser rat trypsin	2213

that the structure of the substrate binding pocket of the mutant might be deformed. This cannot be due to dimerization because even at much higher concentrations than that used for the binding experiments [10] we were unable to detect dimer formation. However, the structure of the monomeric mutant in solution is not necessarily the same as that of the subunits in the crystallized dimer. It is likely that there is structural co-operativity between the two processes: the structural rearrangement around the newly introduced Ser189 promotes dimerization, while dimerization acts toward the structural transition of the activation domain. The structural plasticity of the activation domain in chymotrypsinogen and trypsinogen has long been known [11,29,30] and the two structural isoforms, α and γ, of activated chymotrypsin [2] might also result from a certain amount of variation in the activation domain (reviewed in [7]). Our present study provides the first evidence for the structural plasticity of the activation domain in an activated unliganded trypsin structure. Thus, a further example is added to a series of experimental data indicating that this structural unit of serine proteases is a kind of 'sensory device' that responds differentially to different external or internal signals. Such signals are effects from physiological activation processes [29], crystal packing [30], inhibitor and other ligand binding to the zymogen [11], acyl-enzyme intermediate formation upon the inhibition of trypsin by serpins [32], and finally a point mutation in the activation domain region of trypsin (this study). It is our hypothesis that such, even if slight, enzyme-and/or substrate-specific conformational changes of the activation domain accompany substrate-specific catalysis by serine proteases [28].

ACKNOWLEDGEMENTS

We are grateful to L. N. Johnson (University of Oxford) for the stimulating discussion of this work and for reading and correcting our manuscript. We thank L. Szilágyi for providing the yeast expression system and I. Venekei for helpful consultations during structure analysis. This work was supported by a special grant from the Hungarian Academy of Science to L. G., a grant from the Ministry of Education No. FKFP-B05/1997 to L. G. and a grant from the National Scientific Research Foundation No. OTKA T22191 to G. N.-Sz.

REFERENCES

1. Neurath, L. (1957) The activation of zymogens. In *Advances in Protein Chemistry* (Anfinsen, C.B., Anson, M.L., Bailey, K. & Edsall, J.T., eds), Vol. 12, pp. 319–386. Academic Press, New York.
2. Desnuelle, P. (1960) Chymotrypsin. In *The Enzymes* (Boyer, P.D., Lardy, H. & Myrback, K., eds), Vol. 4, pp. 93–118. Academic Press, New York.
3. Steitz, T.A., Henderson, R. & Blow, D.M. (1969) Structure of crystalline α-chymotrypsin. III. crystallographic studies of substrates and inhibitors bound to the active site of α-chymotrypsin. *J. Mol. Biol.* **46**, 337–348.
4. Stroud, R.M., Kay, L.M. & Dickerson, R.E. (1974) The structure of bovine trypsin: electron density maps of the inhibited enzyme at 5 Å and at 2.7 Å resolution. *J. Mol. Biol.* **83**, 185–208.
5. Fehlhammer, H. & Bode, W. (1975) The refined crystal structure of bovine β-trypsin at 1.8 Å resolution. *J. Mol. Biol.* **98**, 683–693.
6. Perona, J.J. & Craik, C.S. (1995) Structural basis of substrate specificity in the serine proteases. *Protein Sci.* **4**, 337–360.
7. Gráf, L., Szilágyi, L. & Venekei, I. (1998) Chymotrypsin. In *Handbook of Proteolytic Enzymes* (Barrett, A.J., Rawlings, N.D. & Woessner, J.F., eds), pp. 30–38. Academic Press, London.
8. Gráf, L., Jancsó, Á., Szilágyi, L., Hegyi, G., Pintér, K., Náray-Szabó, G., Hepp, J., Medzihradszky, K. & Rutter, W.J. (1988) Electrostatic complementarity within the substrate-binding pocket of trypsin. *Proc. Natl Acad. Sci. USA* **85**, 4961–4965.
9. Perona, J.J., Hedstrom, L., Wagner, R.L., Rutter, W.J., Craik, C.S. & Fletterick, R.J. (1994) Exogenous acetate reconstitutes the enzymatic activity of trypsin Asp189Ser. *Biochemistry* **33**, 3252–3259.
10. Hedstrom, L., Farr-Jones, S., Kettner, C.A. & Rutter, W.J. (1994) Converting trypsin to chymotrypsin: ground-state binding does not determine substrate specificity. *Biochemistry* **33**, 8764–8769.
11. Bode, W., Schwager, P. & Huber, R. (1978) The transition of bovine trypsinogen to a trypsin-like state upon strong ligand binding. *J. Mol. Biol.* **118**, 99–112.
12. Venekei, I., Szilágyi, L., Gráf, L. & Rutter, W.J. (1996) Attempts to convert chymotrypsin to trypsin. *FEBS Lett.* **379**, 143–147.
13. Higashi, T. (1990) A suite of programs for the processing R-AXIS imaging plate data. Rigaku Corp., The Woodlands, TX, USA.
14. Perona, J.J., Tsu, C.A., Craik, C.S. & Fletterick, R.J. (1993) Crystal structure of rat anionic trypsin complexed with the protein inhibitors APPI and BPTI. *J. Mol. Biol.* **230**, 919–933.
15. Navaza, J. (1994) AMoRe: an automated package for molecular replacement. *Acta Crystallogr.* **A50**, 157–163.
16. Collaborative Computing Project, Number 4. (1994) The CCP4 suite: programs for protein crystallography. *Acta Crystallogr.* **D50**, 760–763.
17. Jones, T.A., Zou, J.Y., Cowan, S.W. & Kjeldgaard, M. (1991) Improved methods for building protein models in electron density maps and the location of errors in these models. *Acta Crystallogr.* **A47**, 110–119.
18. Brünger, A.T. (1992) *X-PLOR (Version 3.1), a System for X-Ray Crystallography and NMR.* Yale University Press, New Haven, CT.
19. Laskowski, R.A., MacArthur, M.W., Moss, D.S. & Thornton, J.M. (1993) PROCHECK: a program to check the stereochemical quality of protein structures. *J. Appl. Crystallogr.* **26**, 283–291.
20. Tulinsky, A. & Blevins, R.A. (1987) Structure of a tetrahedral transition state complex of α-chymotrypsin dimer at 1.8 Å resolution. *J. Biol. Chem.* **262**, 7737–7743.
21. Ferrin, T.E., Huang, C.C., Jarvis, L.E. & Langridge, R. (1988) The MIDAS display system. *J. Mol. Graphics* **6**, 13–27.
22. Timasheff, S.N. (1969) On the mechanism of α-chymotrypsin dimerization. *Arch. Biochem. Biophys.* **132**, 165–169.
23. Aune, K.C. & Timasheff, S.N. (1971) Dimerization of α-chymotrypsin. I. pH dependence in the acid region. *Biochemistry* **10**, 1609–1616.
24. Birktoft, J.J. & Blow, D.M. (1972) Structure of α-chymotrypsin. *J. Mol. Biol.* **68**, 187–240.
25. Nicholls, A., Sharp, K. & Honig, B. (1991) Protein folding and association: Insights from the interfacial and thermodynamic properties of hydrocarbons. *Proteins* **11**, 281–296.
26. Hedstrom, L., Szilágyi, L. & Rutter, W.J. (1992) Converting trypsin to chymotrypsin: the role of surface loops. *Science* **255**, 1249–1253.
27. Perona, J.J., Hedstrom, L., Rutter, W.J. & Fletterick, R.J. (1995) Structural origins of substrate discrimination in trypsin and chymotrypsin. *Biochemistry* **34**, 1489–1499.
28. Gráf, L. (1995) Structural basis of serine protease action: the fourth dimension. In *Natural Sciences and Human Thought* (Zwilling, R., ed.), pp. 139–148. Heidelberg, Springer-Verlag.
29. Huber, R. & Bode, W. (1978) Structural basis of the activation and action of trypsin. *Acc. Chem. Res.* **11**, 114–122.
30. Wang, D., Bode, W. & Huber, R. (1985) Bovine chymotrypsinogen A. X-ray crystal structure analysis and refinement of a new crystal form at 1.8 Å resolution. *J. Mol. Biol.* **185**, 595–624.
31. Janin, J. (1997) Specific versus non-specific contacts in protein crystals. *Nat. Struct. Biol.* **4**, 973–974.
32. Kaslik, G., Kardos, J., Szabó, E., Szilágyi, L., Závodszky, P., Westler, M., Markley, J.L. & Gráf, L. (1997) Effect of serpin binding on the target proteinase: global stabilization, localized increased structural flexibility, and conserved hydrogen bonding at the active site. *Biochemistry* **36**, 5455–5464.